Dalton Transactions

Accepted Manuscript

ROYAL SOCIETY OF CHEMISTRY

www.rsc.org/dalton

Solvent-Induced Synthesis of Cobalt(II) Coordination Polymers Based on a Rigid Ligand and Flexible Carboxylic Acid Ligands: Syntheses, Structures and Magnetic Properties

Ting Wang, Chuanlei Zhang, Zemin Ju and Hegen Zheng*

State Key Laboratory of Coordination Chemistry, School of Chemistry and Chemical Engineering, Collaborative Innovation Center of Advanced Microstructures, Nanjing University, Nanjing , 210093, China.

ABSTRACT:

Five new cobalt(II) coordination architectures, $\{[Co(L)_2(H_2O)_2]\cdot 2H_2O\cdot 2NO_3\}_n$ (**1**), $\{[Co(L)(ppda)]\cdot 2H_2O\}_n$ (**2**), $\{[Co_2(L)(ppda)_2]_2\cdot H_2O\}_n$ (**3**), $\{[Co(L)(nba)]\cdot 5H_2O\}_n$ (**4**), $\{[Co(L)(oba)]_2\cdot 3H_2O\}_n$ (**5**), have been constructed from the rigid ligand L [L = 2,8-di(1*H*-imidazol-1-yl)dibenzofuran] and different flexible carboxylic acid ligands [H_2ppda = 4,4'-(perfluoropropane-2,2-diyl)dibenzoic acid, H_2nba = 4,4'-azanediyldibenzoic acid, H_2oba = 4,4'-oxydibenzoic acid]. Depending on the nature of the solvent systems, these five different coordination polymers were synthesized and characterized by single-crystal X-ray diffraction, IR, PXRD and elemental analysis. Compounds **1**, **2** and **3** were obtained by one-pot method, then we utilized the solvent-induced effect to obtain almost pure crystals **1**-**3**, respectively. Compound **1** is an infinite 1D chain which is formed by L ligands and Co atoms. Compound **3** contains a $[Co_2(CO_2)_4]$ secondary building unit (SBU), and can be topologically represented as a 6-connected 2-fold interpenetrating **pcu** net with a point symbol of $\{4^{12}\cdot 6^3\}$. Compound **4** can be characterized as a 4-connected **sql** tetragonal planar network with the point symbol of $\{4^4\cdot 6^2\}$. In compounds **2** and **5**, there are a 1D chain which is formed by flexible carboxylic acid ligands and Co atoms, then the 1D chain is linked by the L ligands in the tilting direction, leading to

the formation of a 2D layer. Furthermore, UV-vis, TGA and magnetic properties studies have been investigated in detail.

INTRODUCTION

In recent years, metal−organic frameworks (MOFs)[1] have attracted intensive attention not only due to their topological varieties but also because of their potential applications as functional materials in the areas of gas adsorption,[2] separation,[3] catalysis,[4] drug delivery,[5] molecular magnetism,[6] photoluminescence[7] and solvatochromism.[8] In general, practical applications of MOFs are directly related to their structural features. To date, however, how to rationally design and synthesize MOFs with the desired structures and properties is still a challenge because the formation of MOFs may be easily affected by many factors. Generally, the structure and topology of coordination polymer generated from transition-metal ‘‘nodes’’ and organic ‘‘spacers’’ can be controlled by selection of ligands, pH, solvents, metal ions, metal-to-ligand ratios, reaction temperature, and counterions and so forth.[9] In particular, the nature of the solvent is an important factor because its structure as well as chemical properties can influence the rate of crystal growth and the final structure.[10] A large number of new MOFs have been constructed with many of the templating molecules showing unprecedented structural characteristics, and in some cases, solvent-induced properties like enhancement of porosity,[11] electrochemical property,[12] catalytic activity,[13] and so forth.

Because configuration, coordination activity and relative orientation of the donor groups of the organic ‘‘spacers’’ take important roles in determining the structure and geometry of the polymers, we have designed and synthesized a rigid ligand L [L = 2,8-di(1*H*-imidazol-1-yl)dibenzofuran]. And then, five cobalt(II) coordination polymers, $\{[Co(L)_2(H_2O)_2]\cdot 2H_2O\cdot 2NO_3\}_n$ (**1**), $\{[Co(L)(ppda)]\cdot 2H_2O\}_n$ (**2**), $\{[Co_2(L)(ppda)_2]_2\cdot H_2O\}_n$ (**3**), $\{[Co(L)(nba)]\cdot 5H_2O\}_n$ (**4**), $\{[Co(L)(oba)]_2\cdot 3H_2O\}_n$ (**5**), were synthesized based on the rigid ligand L and flexible carboxylic acid ligands as the co-ligand under solvothermal conditions, forming different structures of 1D chains, 2D layers and 3D networks. For these five compounds, the structural

formations are effected by using different solvents or different carboxylic acid ligands.

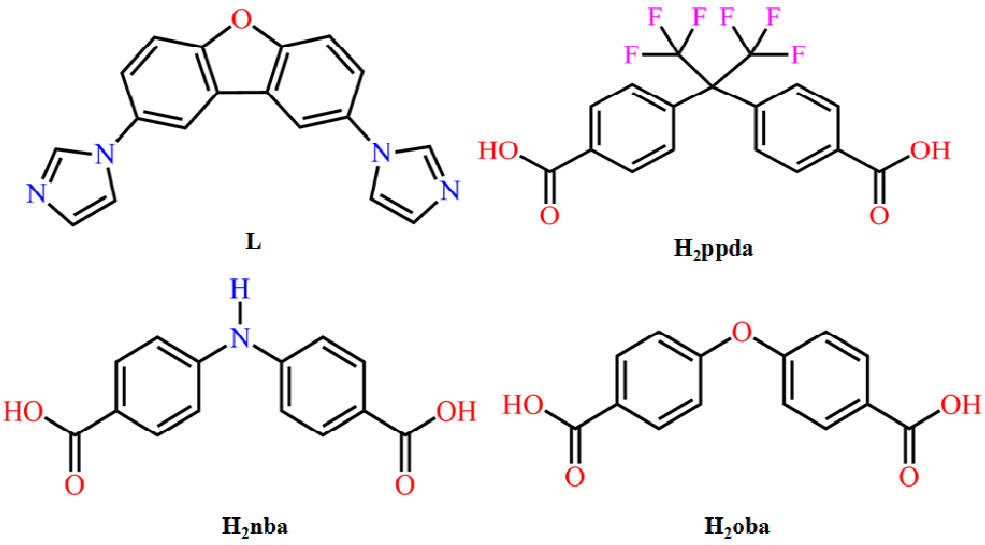

Scheme 1. Structures of the L ligand and flexible carboxylic acid ligands in this work.

EXPERIMENTAL SECTION

Materials and methods. All reagents and solvents except L ligand were purchased from commercial sources and used without further purification. Powder X-ray diffraction (PXRD) patterns were collected in the 2θ = 5-50 ° range with a scan speed of 0.2 deg s^{-1} on a Bruker D8 Advance instrument using Mo Kα radiation at room temperature, in which the X-ray tube was operated at 40 kV and 40 mA. Fourier Transform Infrared (FT-IR) spectra of these complexes were obtained on a Bruker Vector 22 FT-IR spectrophotometer by using KBr pellets. Thermogravimetric analyses (TGA) were performed on a Perkin-Elmer thermal analyzer with a heating rate of 20 °C min^{-1} under a nitrogen atmosphere from room temperature to 800 °C. Solid-state UV-vis diffuse reflectance spectra were obtained at room temperature using Shimadzu UV-3600 double monochromator spectrophotometer, and $BaSO_4$ was used as a 100% reflectance standard for all materials. The temperature-dependent magnetic susceptibility was measured on the SQUID system with 2 kOe external magnetic field.

Synthesis of 2,8-di(1*H*-imidazol-1-yl)dibenzofuran (L). The L ligand was synthesized by a two-step procedure. At first step, the 3,6-dibromo-oxygafluorene was synthesized according to the reported literature.[14]

Then, a mixture of CuI (0.15 g), 3,6-dibromo-oxygafluorene (3 g, 9 mmol), imidazole (1.53 g, 22.5 mmol), and K_2CO_3 (3.11 g, 22.5 mmol) with anhydrous DMF (30 mL) in a 100 mL two-necked round-bottom flask under N_2 was stirred at 150 ^oC for 72 h. The mixture was then cooled to room temperature. Solvent was removed by distillation under a vacuum. The resulting residue was dissolved in $CHCl_3$ (200 mL) and washed thoroughly by water to remove excess imidazole. The organic layer was dried by anhydrous $MgSO_4$ and filtered. The desired compound L was separated by silica gel column chromatography (EA/CH_3OH = 5:1) to afford white powder in a yield of 84%. ^1H NMR (500 MHz, DMSO): δ: 8.48 (d, 2H), 8.28 (s, 2H), 7.90 (d, 2H), 7.84 (dd, 2.4 Hz, 2H), 7.79 (d,2H), 7.18 (s, 2H). ^{13}C NMR (101 MHz, DMSO): δ: 154.70, 135.98, 132.99, 129.95, 124.31, 121.49, 118.77, 113.98, 113.03. IR (KBr, cm^{-1}): 3398(m), 3084(m), 1642(w), 1600(m), 1501(vs), 1458(m), 1429(m), 1305(m), 1240(s), 1193(s), 1110(m), 1045(s), 1021(w), 956(w), 909(m), 856(m), 808(s), 773(m), 726(s), 649(s), 584(w) (Supporting Information, Figures S1, S2 and S3).

Synthesis of compounds 1-5.

Compounds **1**, **2**, **3** are obtained by one-pot method using DMF/CH_3CN/H_2O (1:1:1, v/v/v), and then we utilized the solvent-induced effect to obtain almost pure crystals, respectively. The yield of the reaction was ca. 40% for compound **1**, ca. 20% for compound **2** and ca. 10% for compound **3** based on L ligand.

Synthesis of $\{[Co(L)_2(H_2O)_2]\cdot 2H_2O\cdot 2NO_3\}_n$ (1). A mixture of $Co(NO_3)_2\cdot 6H_2O$ (29.1 mg, 0.1 mmol), L (30 mg, 0.1 mmol) was dissolved in 3 mL of DMF/H_2O (1:2, v/v). The final mixture was placed in a Parr Teflon-lined stainless steel vessel (15 mL) under autogenous pressure and heated at 95 °C for 3 days. Orange-block crystals were obtained. The yield of the reaction was ca. 80% based on L ligand. Calcd for $C_{36}H_{32}CoN_{10}O_{12}$: C, 50.49%; H, 3.74%; N, 16.36%. Found: C, 50.47%; H, 3.72%; N,

16.35%. IR (KBr, cm^{-1}): 3402(vs), 3125(w), 1643(m), 1513(s), 1395(m), 1309(m), 1203(m), 1108(m), 1061(m), 934(w), 818(m), 661(m), 590(w).

Synthesis of $\{[Co(L)(ppda)]\cdot 2H_2O\}_n$ (2). A mixture of $Co(NO_3)_2\cdot 6H_2O$ (29.1 mg, 0.1 mmol), L (30 mg, 0.1 mmol) and H_2ppda (39.2 mg, 0.1 mmol) was dissolved in 6 mL of DMF/H_2O (2:4, v/v). The final mixture was placed in a Parr Teflon-lined stainless steel vessel (15 mL) under autogenous pressure and heated at 95 °C for 3 days. Purple needle-shaped crystals were obtained. The yield of the reaction was ca. 70% based on L ligand. Calcd for $C_{35}H_{24}CoF_6N_4O_7$: C, 53.49%; H, 3.06%; N, 7.13%. Found: C, 53.47%; H, 3.03%; N, 7.15%. IR (KBr, cm^{-1}): 3048(s), 1666(w), 1592(vs), 1539(m), 1515(vs), 1399(vs), 1227(vs), 1196(m), 1109(m), 967(w), 874(m), 818(m), 749(m), 696(w).

Synthesis of $\{[Co_2(L)(ppda)_2]_2\cdot H_2O\}_n$ (3). A mixture of $Co(NO_3)_2\cdot 6H_2O$ (29.1 mg, 0.1 mmol), L (30mg, 0.1 mmol) and H_2ppda (39.2 mg, 0.1 mmol) was dissolved in 4 mL of DMF/CH_3CN/H_2O (1:1:2, v/v/v). The final mixture was placed in a Parr Teflon-lined stainless steel vessel (15 mL) under autogenous pressure and heated at 95°C for 3 days. Dark purple block crystals were obtained. The yield of the reaction was ca. 54% based on L ligand. Calcd for $C_{104}H_{58}Co_4F_{24}N_8O_{19}$: C, 51.67%; H, 2.40%; N, 4.64%. Found: C, 51.61%; H, 2.44%; N, 4.61%. IR (KBr, cm^{-1}): 3411(m), 1629(vs), 1512(m), 1404(vs), 1253(m), 1169(v), 1115(m), 1060(w), 843(m), 778(w), 650(w).

Synthesis of $\{[Co(L)(nba)]\cdot 5H_2O\}_n$ (4). A mixture of $Co(NO_3)_2\cdot 6H_2O$ (29.1 mg, 0.1 mmol), L (30 mg, 0.1 mmol) and H_2nba (25.7 mg, 0.1 mmol) was dissolved in 4 mL of DMF/H_2O (1:3, v/v). The final mixture was placed in a Parr Teflon-lined stainless steel vessel (15 mL) under autogenous pressure and heated at 95 °C for 3 days. Purple block crystals were obtained. The yield of the reaction was ca. 70% based on L ligand. Calcd for $C_{32}H_{31}CoN_5O_{10}$: C, 54.50%; H, 4.40%; N, 9.94%. Found: C, 54.51%; H, 4.42%; N, 9.95%. IR (KBr, cm^{-1}): 3390(m), 1662(m), 1591(vs), 1509(vs), 1391(vs), 1327(v), 1245(m), 1203(m), 1173(m), 1111(m), 1056(m), 936(w), 812(w), 781(m), 697(w), 657(m), 503(w).

Synthesis of {[Co(L)(oba)]$_2$·3H$_2$O}$_n$ (5). A mixture of $Co(NO_3)_2·6H_2O$ (29.1 mg, 0.1 mmol), L (30 mg, 0.1 mmol) and H_2oba (25.8 mg, 0.1 mmol) was dissolved in 6 mL of DMF/H_2O (2:4, v/v). The final mixture was placed in a Parr Teflon-lined stainless steel vessel (15 mL) under autogenous pressure and heated at 95 °C for 3 days. Purple block crystals were obtained. The yield of the reaction was ca. 90% based on L ligand. Calcd for $C_{64}H_{46}Co_2N_8O_{15}$: C, 59.77%; H, 3.58%; N, 8.72%. Found: C, 59.76%; H, 3.61%; N, 8.71%. IR (KBr, cm^{-1}): 3408(s), 1666(m), 1592(vs), 1539(s), 1515(vs), 1399(vs), 1227(vs), 1196(m), 1159(m), 1109(m), 1059(m), 967(w), 941(w), 847(m), 818(m), 783(m), 749(w), 696(m), 655(w), 593(w).

Single Crystal X-ray Studies. Crystallographic data of **1-5** were collected on a Bruker Smart Apex CCD diffractometer with graphite monochromated Mo Kα radiation (λ = 0.71073 Å) using the ω-scan technique. The linear absorption coefficients, scattering factors for the atoms, and the anomalous dispersion corrections were referred to from the International Tables for X-ray Crystallography. Semiempirical absorption correction was carried by using the SADABS program.[15] The structures were solved by direct methods, and all non-hydrogen atoms were refined anisotropically on F^2 by the full-matrix least-squares technique using the SHELXL-97 crystallographic software.[16] The hydrogen atoms were positioned geometrically by using a riding model. The contribution of the electron density by the remaining disorder solvent molecule in the channels of **4** was partially removed by the SQUEEZE routine in PLATON.[17] We have many attempts to obtain **4**, but the crystal data of **4** are not good. Details of the crystal parameters, data collection, and refinements for **1-5** are summarized in Table 1. Selective bond distances and angles are given in Table S1 (Supporting Information). The topological analysis and some diagrams were produced using the TOPOS program.[18]

RESULTS AND DISCUSSION

Crystal Structure of $\{[Co(L)_2(H_2O)_2]\cdot 2H_2O\cdot 2NO_3\}_n$ (1). Single-crystal X-ray structural analysis reveals that the structure of **1** is composed of a 1D chain and crystallizes in a monoclinic system with space group *C*2/*c*. As shown in Fig. 1a, the asymmetric unit contains half a Co atom, one L ligand, one coordinated water molecule, and one lattice water, one free nitrate anion. In compound **1**, each Co(II) atom is surrounded by four nitrogen atoms from four L ligands and two oxygen donors from two coordinated water molecules to adopt an octahedral geometry. The axial positions of the octahedron are occupied by O(1) and O(2) with an O(1)-Co(1)-O(2) angle of 180 °. The bond distances of Co(1)-O(1) and Co(1)-O(2) are 2.089(2) and 2.104(2) Å, respectively. Four N atoms {N(1)#1, N(1)#2, N(3), N(3)#} lie in the equatorial plane. The distances of the Co-N bonds are from 2.1480(4) to 2.1492(3) Å. The bond angle of N-Co-O is in the ranges of 88.59(4)°-91.41(4)°. The bond angles of N(1)#2-Co(1)-N(1)#1 and N(3)#3-Co(1)-N(3) are 177.35(10)° and 177.19(9)°, respectively. Two L ligands link two Co(II) cations to form an approximately rhombus $[Co_2(L)_2]$ 26-membered metallamacrocycle (Fig. 1c). The supplementary interior angles are 75.595° and 104.405°, respectively.

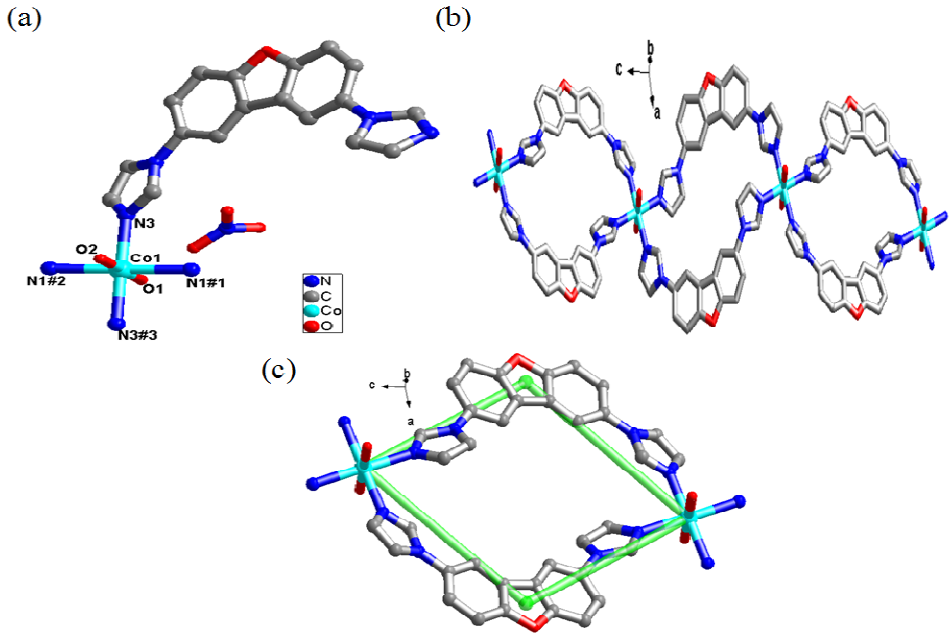

Fig. 1 (a) Coordination environment of the Co(II) cation in **1**. The hydrogen atoms are omitted for clarity. Symmetry codes: #1 = − *x*, − *y*, − *z*; #2 = *x*, − *y*, *z* + 1/2; #3 = − *x*, *y*, −*z* + 1/2. (b) An infinite 1D chain formed by the L ligand and the Co(II) cations. (c) Rhombus $[Co_2(L)_2]$ metallamacrocycle.

Crystal Structure of $\{[Co(L)(ppda)]\cdot 2H_2O\}_n$ (2). Compound **2** crystallizes in the monoclinic crystal system of $P2_1/c$ space group. Its asymmetric unit consists of one Co atom, one L ligand, one $ppda^{2-}$ anion, and two lattice water molecules. Each Co(II) is coordinated by two nitrogen atoms from two L ligands and two carboxylate oxygen atoms from two $ppda^{2-}$ ligands to form a tetrahedral coordination configuration (Fig. 2a). The Co-O bond distances are 1.965(2) and 1.966(2) Å, and the Co-N bond distances are 1.997(3) and 2.016(3)Å; the O-Co-O angle is 100.75(10)°, N-Co-N angle is 116.48(11)°, and the N-Co-O angles are in the range of 101.67(10)-112.42(10)°. There is one 1D chain which is constructed from $ppda^{2-}$ ligands and Co(II) atoms in the structure (Fig. 2b), the Co···Co distance is 13.911(1) Å. Such 1D *zig-zag* chain is linked by the L ligand in the tilting direction, leading to the formation of a 2D layer (Fig. 2c). Two L ligands link two Co(II) cations to form an approximately rhombus $[Co_2(L)_2]$ 26-membered metallamacrocycle. The supplementary interior angles are 88.642° and 91.358°, respectively (Fig. 2d). From the topological perspective, the framework of **2** can be topologically represented as a 3-connected net **hcb** hexagonal planar net with point symbol $\{6^3\}$ (Fig. 2e).

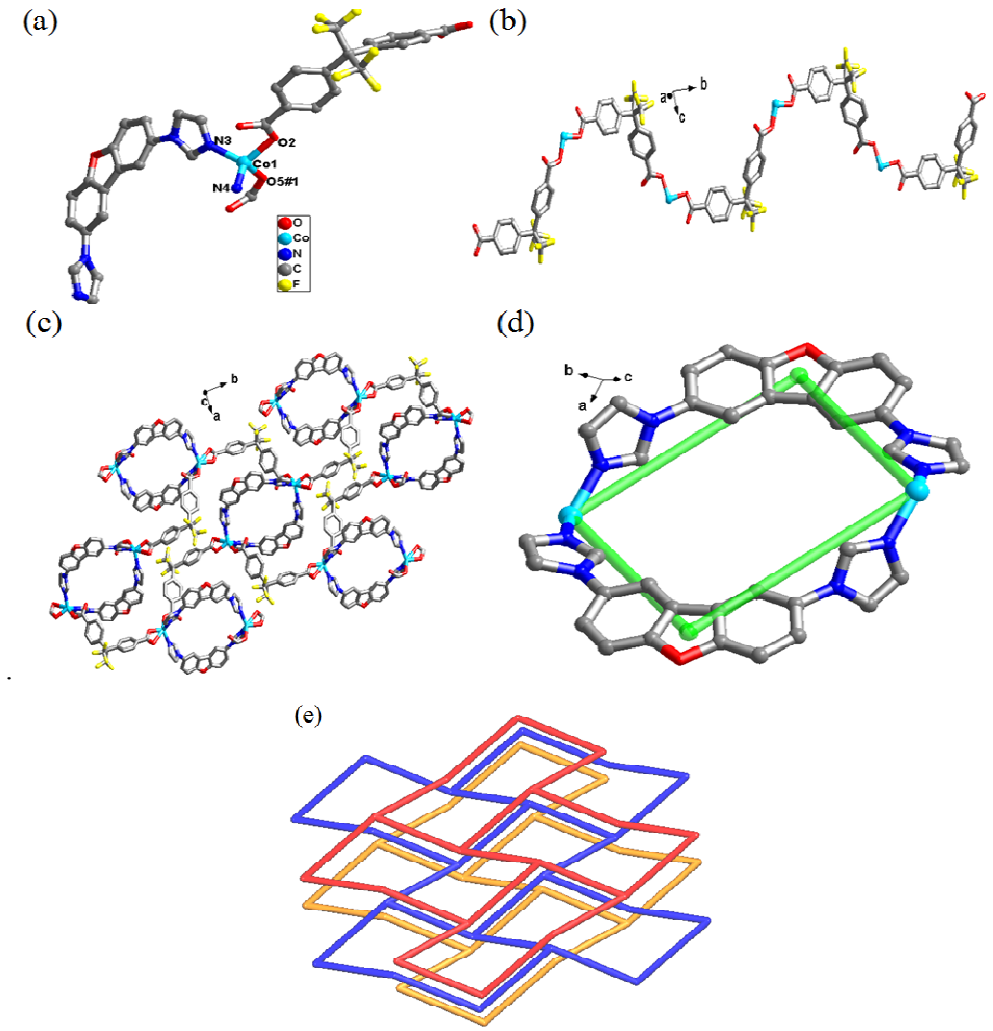

Fig. 2 (a) Coordination environment of the Co(II) cation in **2**. The hydrogen atoms are omitted for clarity. Symmetry codes: #1 = − *x* + 2, *y* − 1/2, − *z* + 3/2. (b) An infinite 1D chain formed by the ppda^{2-} ligand and the Co(II) cations. (c) 2D network of **2**. (d) Rhombus [$Co_2(L)_2$] metallamacrocycle. (e) Schematic view of the **hcb** topology of **2**.

Crystal Structure of {[Co_2(L)(ppda)$_2$]$_2$·H_2O}$_n$ (3). The single crystal X-ray diffraction analysis reveals that the compound **3** is a 3D supramolecular structure and crystallizes in *P*2/*c* space group. The asymmetric unit contains one Co atom, half a L, one completely deprotonated ppda ligand, and a quarter of lattice water molecule. The coordination environment around the Co(II) cation is exhibited in Fig. 3a. Each Co(II) is square-pyramidally coordinated by four carboxylate oxygen atoms from four ppda ligands at the basal positions and one nitrogen atom from one L ligand at the apical

position. The Co-N bond distance is 2.0567(16) Å, and the Co-O bond distances vary in the range of 2.0196(14)-2.1169(14) Å; the N-Co-O angles are from 92.05(6)° to 106.09(7)°, and the O-Co-O angles are in the range of 106.09(7)-161.01(6)°. Two crystallographically equivalent Co(II) cations are bridged by four carboxylate groups adopting a bis-bidentate coordination mode to generate a distorted dinuclear Co(II) "paddle-wheel" secondary building unit [$Co_2(CO_2)_4$], with a Co···Co distance of 2.9066(5) Å. And "paddlewheel" is bridged with ppda ligands to form a 2D flat network with quadrangle grids. On a careful look at the geometry of the 2D layer, it was observed that left- and right- handed 1D helical chains coexist and array alternately by sharing the paddlewheel SBUs (Fig. 3b). The layers are interconnected to form a 3D structure via L ligands with a Co···Co distance of 15.5050 Å (Fig. 3c). Better insight into the complicated 3D architecture can be achieved by topology analysis, so the resulting structure can be reduced to a 6-connected 2-fold interpenetrating **pcu** net with a point symbol of $\{4^{12}\cdot6^3\}$ by simplifying the L and 4,4′-sdb as linkers. In order to minimize the large voids in the single net, two equivalent nets adopt 2-fold interpenetration (Fig. 3d).

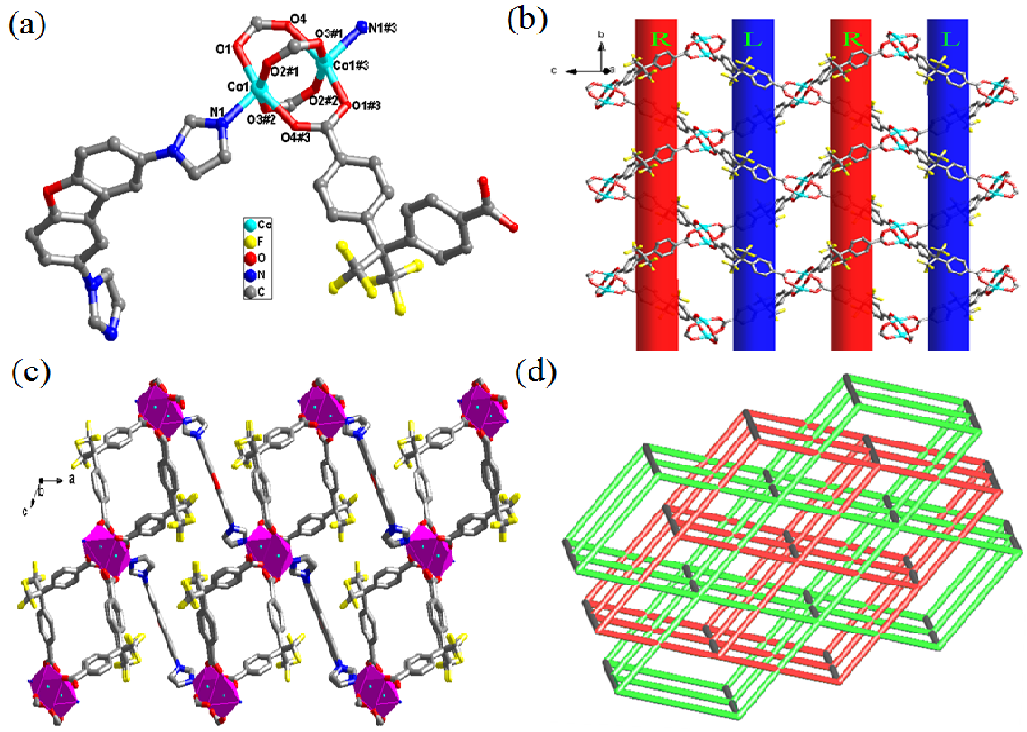

Fig. 3 (a) Coordination environment of the Co(II) cations in **3**. The hydrogen atoms are omitted for clarity. Symmetry codes: #1 = x, $-y+1$, $1/2+z$; #2 = $1-x$, $y-1$, $-z+3/2$; #3: $-x+1$, $-y$, $z+2$. (b) Schematic representation of the left-handed and right-handed helical chains in the 2D network constructed from ppda ligands and Co(II) cations in **3**. (c) View of the 3D framework. (d) Schematic view of the 2-fold interpenetrated **pcu** topology of **3**.

Crystal Structure of $\{[Co(L)(nba)]\cdot 5H_2O\}_n$ (4). Compound **4** crystallizes in the monoclinic space group $C2/c$. Its asymmetric unit consists of one crystallographically Co(II) ion, one L ligand, one deprotonated nba ligand and five solvent water molecule. Four lattice water molecules were removed by the SQUEEZE routine in PLATON. Each Co(II) is coordinated by three carboxylate oxygen atoms from three nba ligands in a flat position, and two nitrogen atoms from two L ligands in the axial direction plane, which forms trigonal bipyramid coordination mode (Fig. 4a). The Co-N bond distances are 2.099(4) and 2.118(5) Å, and the Co-O bond distances are 2.047(3), 2.101(4) and 2.105(4) Å; the N-Co-O angles are in the range of 87.45(16)-96.45(18)°, and the O-Co-O angles are in the range of 93.31 (17)-134.72 (16)°. Two crystallographically equivalent Co(II) cations are bridged by two carboxylate groups adopting a bis-bidentate coordination mode to generate a dinuclear Co(II) SBU with a Co···Co distance of 3.5028 Å. Each $[Co_2(CO_2)_2]$ SBU bridges nba ligand to yield one infinite 1D linear chain. And, the other infinite 1D linear chain was generated by L ligands and the Co(II) cations (Fig. 4b). Then, the two types of 1D chains are linked each other to generate a 2D network (Fig. 4b, 4c).

It can be regarded the binuclear cobalt as a network node, thus, the 2D coordination polymer can be characterized as a 4-connected **sql** network with the point symbol of $\{4^4\cdot 6^2\}$ (Fig. 4d).

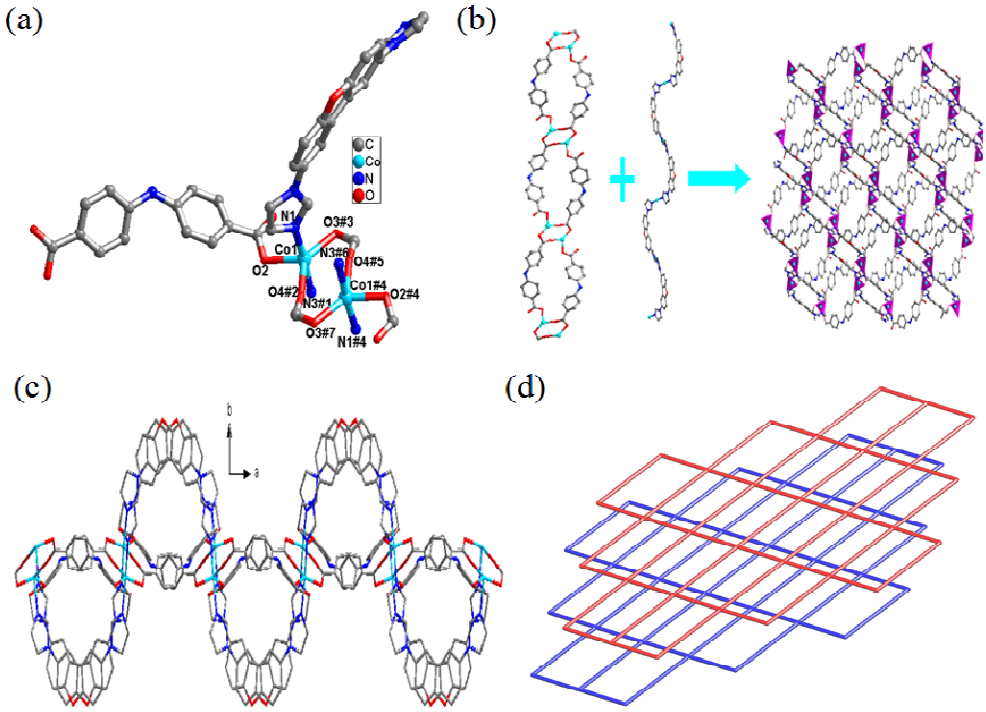

Fig. 4 (a) Coordination environment of the Co(II) cations in **4**. The hydrogen atoms are omitted for clarity. Symmetry codes: #1 = $x - 1/2, -y + 1/2, -1/2 + z$; #2 = $-x, y, -z + 1/2$; #3 = $x + 1/2, -y + 1/2, z - 1/2$; #4 = $-x + 1/2, -y + 1/2, -z$; #5 = $x + 1/2, -y + 1/2, z - 1/2$; #6 = $-x + 1, y, -z + 1/2$; #7 = $-x, y, -z + 1/2$; (b) Left: an infinite 1D linear chain formed by Co(II) cations and nba ligands. Middle: an infinite 1D linear chain constructed from the L ligands and the Co(II) cations. Right: 2D network of **4**. (c) 2D network of 4 from *c* axis direction. (d) Schematic view of **sql** topology of **4**.

Crystal Structure of $\{[Co(L)(oba)]_2 \cdot 3H_2O\}_n$ (5). X-ray diffraction reveals that compound **5** crystallizes in the monoclinic crystal system of *C*2/*c* space group. Its asymmetric unit consists of one Co atom, one L ligand, one oba^{2-} anion, and one and a half lattice water. Each Co(II) is coordinated by two nitrogen atoms from two L ligands and four carboxylate oxygen atoms from two oba^{2-} ligands (Fig. 5a). The Co-O bond distances are from 2.070(2) to 2.237(2)Å, and the Co-N bond distances are 2.063(2) and 2.076(2)Å; the O-Co-O angle are in the range of 59.12(8)-163.66(10)°, N-Co-N angle is 94.48(10)°, and the N-Co-O angles are in the range of 91.97(9)-155.78(9)°. Similar to compound 2, there is one chain in the structure which is constructed from oba^{2-} ligands and Co(II) cations, the Co···Co distance is 14.1947(15) Å and a Co···Co···Co angle of 180°(Fig. 5b). Such 1D chain

is linked by L in the tilting direction, leading to the formation of a 2D framework (Fig. 5c). Two L ligands link two Co(II) cations to form an approximately rhombus $[Co_2(L)_2]$ 26-membered metallamacrocycle (Fig. 5d). The supplementary interior angles are 75.739° and 85.438°, respectively. From the topological perspective, the framework of **5** can be topologically represented as a 3-connected net with point symbol $\{8^2 \cdot 10\}$ (Fig. 5e).

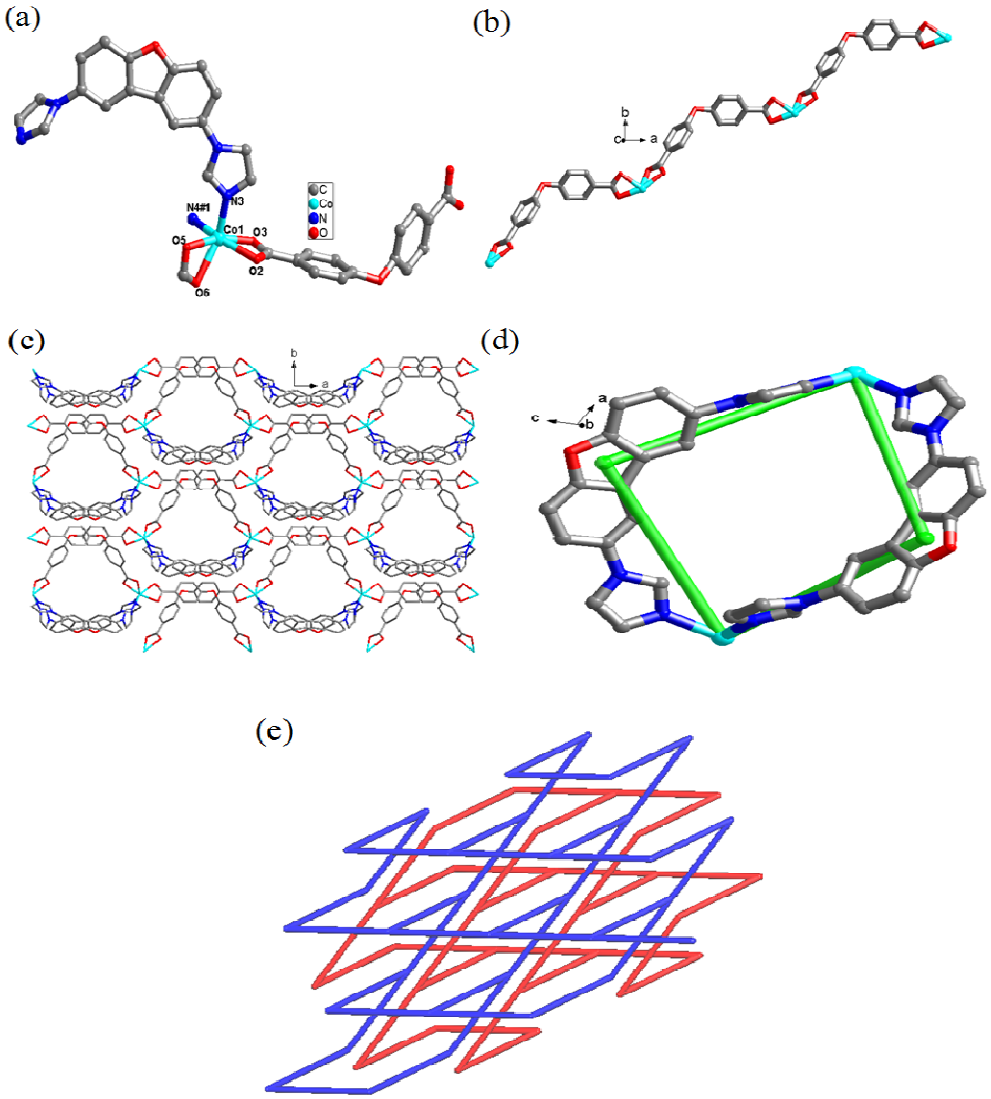

Fig. 5 (a) Coordination environment of the Co(II) cations in **5**. The hydrogen atoms are omitted for clarity. Symmetry codes: #1 = − *x* + 1, *y*, − *z* + 1/2; (b) an infinite 1D linear chain formed by Co(II) cations and oba ligands. (c) 2D network of **5** from *c* axis direction; (d) Rhombus $[Co_2(L)_2]$ metallamacrocycle; (e) Schematic view of 3-connected net topology of **5**.

Effect of different solvents and ligands on supramolecular structures. Compounds **1**, **2** and **3** were obtained by one-pot method, then we chose different ratios of DMF/CH_3CN/H_2O and obtained almost pure crystals **1-3**, respectively. Compound **1** is an infinite 1D chain; compound **2** is a 2D layer network; compound **3** is a 6-connected 2-fold interpenetrating net. The versatility of different solvent composition plays a vital important role in the formation of the structural diversity (Fig. 6).

When we changed the co-ligand H_2ppda to H_2nba and H_2oba, compounds **4** and **5** were obtained. Compound **4** is a 2D layer with $[Co_2(CO_2)_2]$ SBU and can be characterized as a 4-connected **sql** network. Compounds **5** can be topologically represented as a 3-connected net with point symbol $\{8^2 \cdot 10\}$. Different flexible carboxylic acid ligands have a great influence on the structural construction, which may be the main reason for the structural difference in **4** and **5**.

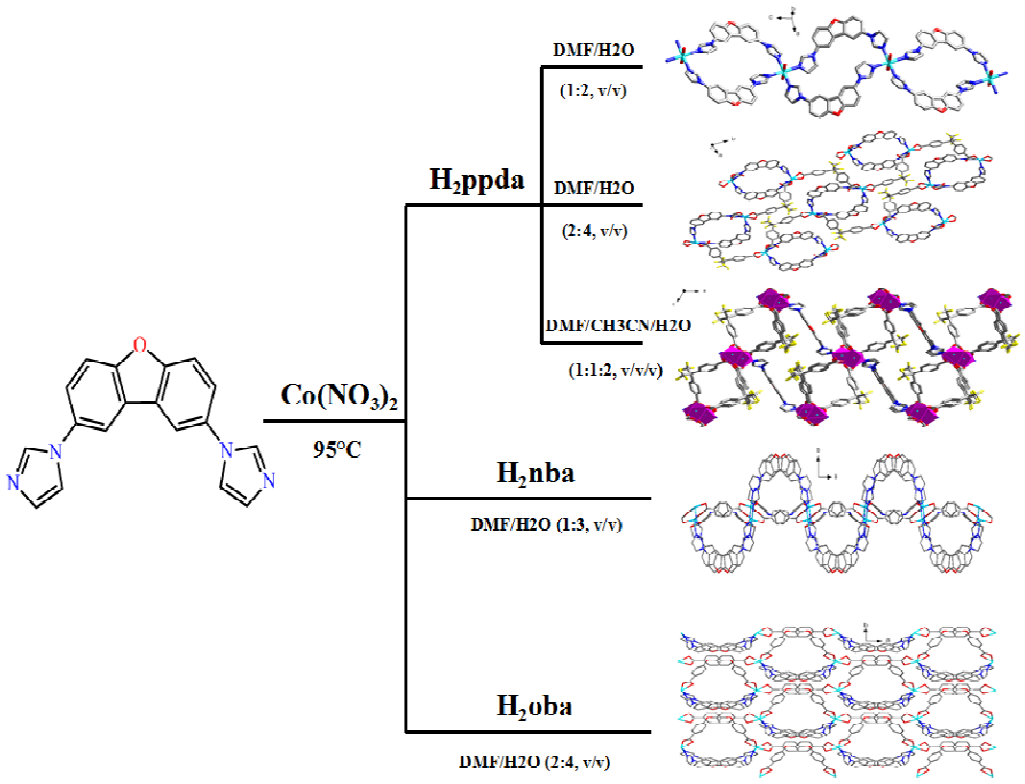

Fig. 6 Structural diversity of compounds **1-5**.

X-ray powder diffraction results. From the PXRD patterns of compounds **1-5** (Supporting Information, Figures S5-S9), the peak positions are agree well with their simulated ones, which indicates that the products have been successfully obtained as pure crystalline phases.

UV-visible spectra. The UV-vis absorption spectra of L, H_2ppda, H_2nba, H_2oba and compounds **1-5** were carried out in the crystalline state at room temperature (Fig. 7). Compounds **1-5** exhibit a narrow absorption band in the range 200-380 nm, which can be ascribed to π-π* transitions of the ligands. Besides this absorption band, for compounds **1**, **3** and **5**, we observe two additional peaks at 430 nm [$^4T_{1g}(F) \rightarrow {}^4T_{2g}(F)$] with a shoulder at 580 nm [$^4T_{1g}(F) \rightarrow {}^4T_{1g}(P)$] and 730 nm assigned to the $^4T_{1g}(F) \rightarrow {}^4A_{2g}(F)$ transitions. For compound **2** and **4**, we observe additional peaks at 500 nm [$^4T_{1g}(F) \rightarrow {}^4T_{2g}(F)$] with a shoulder at 620 nm assigned to the [$^4A_{2g}(F) \rightarrow {}^4T_{2g}(P)$] transition. The higher energy bands can be considered as metal-to-ligand charge-transfer (MLCT) transitions. The lower energy band can be attributed to the spin-allowed d-d electronic transitions of the d^7 (Co^{2+}) cation.[19]

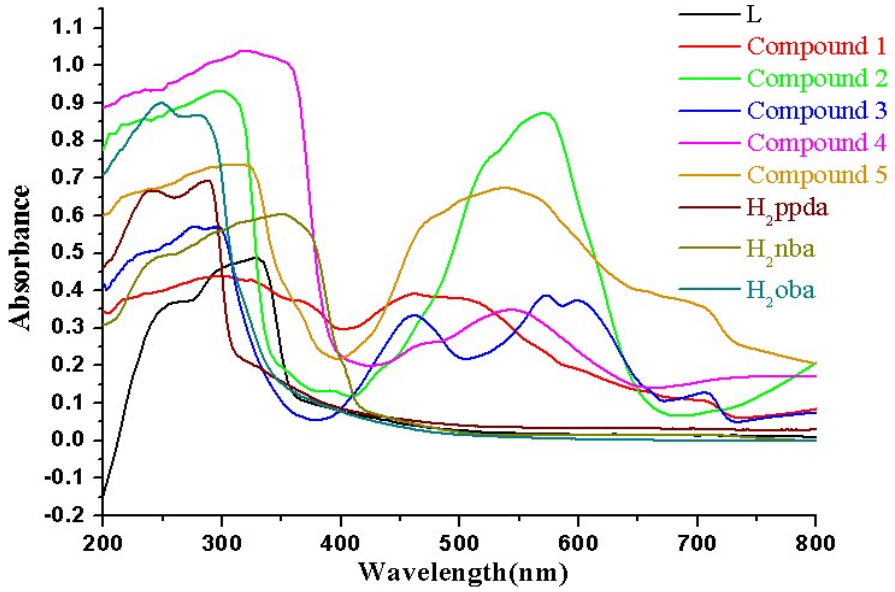

Fig. 7 UV-vis absorbance spectra.

Thermogravimetric analyses. To examine the thermal stabilities of these compounds, TG analyses were carried out (Fig. 8). For compound **1**, a weight loss is observed from ambient temperature to 235 °C due to the release of two lattice water molecules and two coordinated waters with a weight loss of 8.27% (calcd 8.41%). Then the structure was decomposed since 330°C. In the case of **2**, a weight loss of 2.39% from ambient temperature to 102 °C corresponds to the loss of one lattice water (calcd 2.31%). Then the TG curve presents a platform and the framework starts to decompose at 400 °C. The TGA study of compound **3** indicates no obvious weight loss from 20 to 450 °C, suggesting that the frameworks are thermally stable. TGA curve of **4** indicates that there is an initial weight loss of approximate 13.53% between 20 and 360 °C, corresponding to the loss of five lattice water (calcd 12.78%). In the case of **5**, a little weight loss is observed from ambient temperature to 99 °C due to the release of three lattice water molecules, with a weight loss of 4.26% (calcd 4.21%); furthermore, the decomposition of **5** occurs after 420 °C.

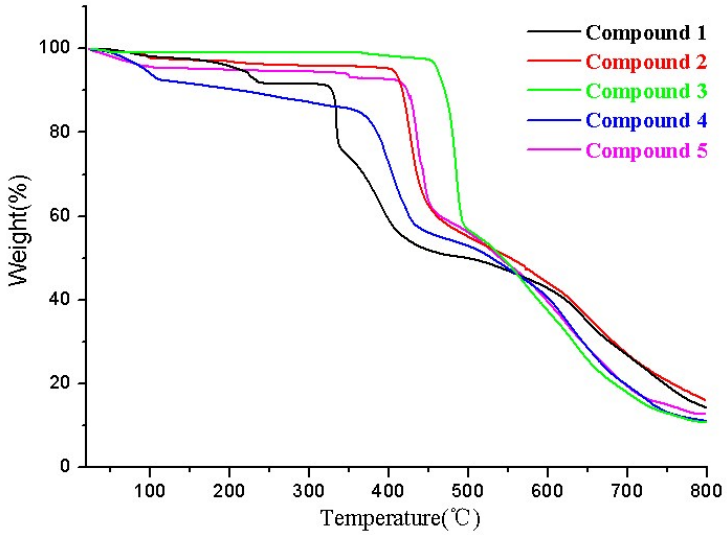

Fig. 8 The TGA curves of **1**-**5**.

Magnetic properties. The temperature-dependent magnetic susceptibilities of **3** and **4** were measured in an applied field of 2000 Oe from 1.8 to 300 K. The $\chi_M T$ and $1/\chi_M$ versus T plots are showing in Fig. 9 and 10, respectively.

As shown in Fig. 9, for compound **3** which contains $[Co_2(CO_2)_4]$ SBU, the $1/\chi_M$ versus T plot can be fitted by the Curie–Weiss law $\chi_M = C/(T-\theta)$, giving a Curie constant C = 9.91 cm^3 K mol^{-1} and Weiss constant $\theta = -5.02$ K. The negative value of θ indicates an antiferromagnetic interaction for **3**. At room temperature the $\chi_M T$ value is 8.87 cm^3 K mol^{-1}, which is larger than the expected 3.875 cm^3 K mol^{-1} for two high-spin isolated Co(II) ions with S = 3/2, indicating that an important orbital contribution is involved.[20] With a decrease of temperature,the $\chi_M T$ value decreases slowly and then rapidly to 0.72 cm^3 K mol^{-1} at 1.8 K, suggesting an antiferromagnetic interaction.

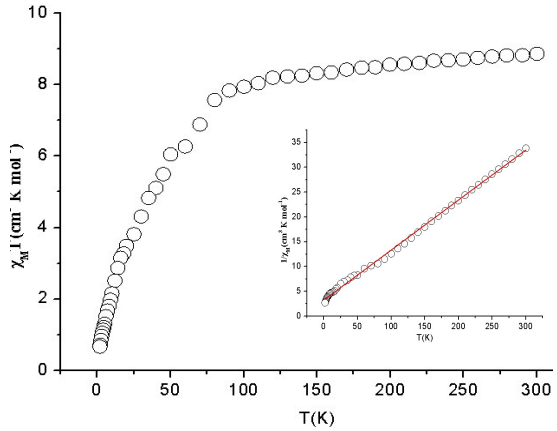

Fig. 9 (a) Experimental magnetic data plotted as $\chi_M T$ versus T for **3**; (b)the inset showing $1/\chi_M$ versus T. The solid line results from a least-squares fit of the data to the theoretical equations.

For compound **4**, the value of $\chi_M T$ at 300 K is 5.24 cm^3 K mol^{-1}, which is larger than the expected 3.875 cm^3 K mol^{-1} for two high-spin isolated Co(II) ions with S = 3/2, suggesting that the effect of spin-orbit coupling known for Co(II) ions.[21] Upon cooling, the $\chi_M T$ value decreases first slowly and then rapidly to avalue of 0.53 cm^3 K mol^{-1} at 1.8 K. The inverse molar magnetic susceptibility plot as a function of temperature is linear, following the Curie–Weiss law with Weiss constant $\theta = -21.69$ K and Curie constant C = 5.65 cm^3 K mol^{-1}. The total decrease of the $\chi_M T$ and the negative θ values indicates that there are antiferromagnetic coupling interactions between the dimeric Co(II) ions or the orbital angular momentum.

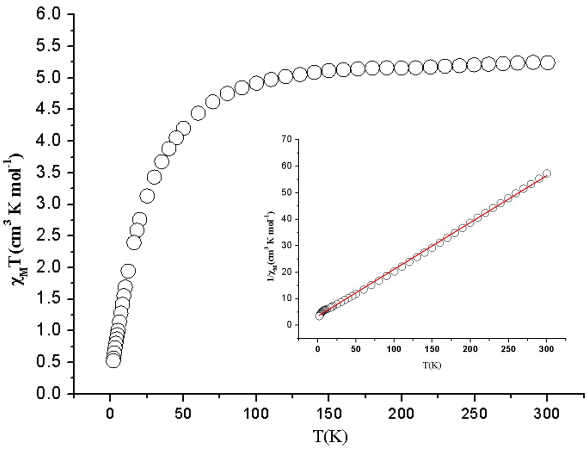

Fig. 10 (a) Experimental magnetic data plotted as $\chi_M T$ versus T for **4**; (b)the inset showing $1/\chi_M$ versus T. The solid line results from a least-squares fit of the data to the theoretical equations.

CONCLUSIONS

In summary, five metal-organic frameworks have been successfully synthesized based on the reaction of the rigid ligand L in the presence of different flexible carboxylic acid ligands and cobalt(II) ions. Compounds **1**, **2**, **3** are obtained by one-pot method, then, we utilized the solvent-induced effect to obtain almost pure crystals, respectively. Compound **1** is an infinite 1D chain, whereas compound **2** is a 2D layer. And compound **3** can be topologically represented as a 6-connected 2-fold interpenetrating **pcu** net with point symbol $\{4^{12}\cdot 6^3\}$. In compound **3**, it is observed that left- and right-handed 1D helical chains coexist and array alternately by sharing the paddlewheel SBUs. We find that the versatility of different solvent composition plays a vital important role in the formation of the structural diversity. When we changed the co-ligand H_2ppda to H_2nba and H_2oba, compounds **4** and **5** were obtained. Compound **4** can be characterized as a 4-connected **sql** planar network. In compounds **5**, there is a 1D chain which is formed by flexible carboxylic acid ligands and Co atoms, then the 1D chain is linked by the L ligand in the tilting direction, leading to the formation of a 2D framework. Among all compouds above, compounds **1**, **2** and **5** contain an approximately rhombus $[Co_2(L)_2]$ 26-membered metallamacrocycle. The magnetism studies show that both **3** and **4** exhibit antiferromagnetic interactions.

SUPPLEMENTARY INFORMATION

PXRD, IR, NMR, the selected bond lengths and angles. CCDC: 1047954-1047958 for **1-5**. For ESI and crystallographic data in CIF or other electronic format see DOI: 10.1039/

ACKNOWLEDGMENT

This work was supported by grants from the Natural Science Foundation of China (Nos. 21371092, 91022011) and National Basic Research Program of China (2010CB923303).

REFERENCES

1. (a) M. O'Keeffe and O. M. Yaghi, *Chem. Rev*., 2012, **112**, 675; (b) N. L. Rosi, J. Eckert, M. Eddaoudi, D. T. J. Kim, M. O'Keefe and O. M. Yaghi, *Science,* 2003, **300**, 1127; (c) M. J. Zaworotko, *Nature,* 2008, **451**, 410; (d) D. Bradshaw, J. E. Warren and M. J. Rosseinsky, *Science,* 2007, **315**, 977.
2. (a) M. P. Suh, H. J. Park, T. K. Prasad and D. W. Lim, *Chem. Rev.,* 2012, **112**, 782; (b) P. Kanoo, S. K. Reddy, G. Kumari, R. Haldar, C. Narayana, S. Balasubramanian and T. K. Maji, *Chem. Commun.,* 2012, **48**, 8487; (c) Z. J. Lin, Y. B. Huang, T. F. Liu, X.Y. Li and R. Cao, *Inorg. Chem.*, 2013, **52**, 3127; (d) D. Kim and H. Lee, *RSC Adv.,* 2015, **5**, 2749.
3. (a) J. R. Li, J. Sculley and H. C. Zhou, *Chem. Rev.,* 2012, **112**, 869; (b) P. Li, Y. He, J. Guang, L. Weng, J. C. Zhao, S. Xiang and B. Chen, *J. Am. Chem. Soc.,* 2014, **136**, 547; (c) X. Z. Luo, X. J. Jia, J. H. Deng, J. L. Zhong, H. J. Liu, K. J. Wang and D. C. Zhong, *J. Am. Chem. Soc.,* 2013, **135**, 11684.
4. (a) J. M. Roberts, B. M. Fini, A. A. Sarjeant, O. K. Farha, J. T. Hupp and K. A. Scheidt, *J. Am. Chem. Soc.,* 2012, **134**, 3334; (b) Y. Zhu, Y. M. Wang, S. Y. Zhao, P. Liu, C. Wei, Y. L. Wu, C. K. Xia and J. M. Xie, *Inorg. Chem.,* 2014, **53**, 7692;

(c) L. H. Wang, Y. Zeng, A. G. Shen, X. D. Zhou and J. M. Hu, *Chem. Commun.*, 2015, **51**, 2052.

5. (a) J. An, S. J. Geib and N. L. Rosi, *J. Am. Chem. Soc.,* 2009, **131**, 8376; (b) D. Cunha, M. B. Yahia, S. Hall, S. R. Miller, H. Chevreau, E. Elkaïm, G. Maurin, P. Horcajada and C. Serre, *Chem. Mater.,* 2013, **25**, 2767; (c) C. B. He, K. D. Lu, D. M. Liu and W. B. Lin, *J. Am. Chem. Soc.,* 2014, **136**, 5181.
6. (a) T. Ma, M. X. Li, Z. X. Wang, J. C. Zhang, M. Shao and X. He, *Cryst. Growth Des*., 2014, **14**, 4155; (b) H. Tan, S. Du, Y. Bi and W. Liao, *Inorg. Chem.,* 2014, **53**, 7083; (c) T. D. Keene, M. J. Murphy, J. R. Price, N. F. Sciortino, P. D. Southon and C. J. Kepert, *Dalton Trans*., 2014, **43**, 14766; (d) L. Chen, J. Wang, J. M. Wei, W. Wernsdorfer, X. T. Chen, Y. Q. Zhang, Y. Song and Z. L. Xue, *J. Am. Chem. Soc.,* 2014, **136**, 12213.
7. (a) Y. Cui, Y. Yue, G. Qian and B. Chen, *Chem. Rev.,* 2012, **112**, 1126; (b) Y. Z. Tang, M. Zhou, J. Huang, Y. H. Tan, J. S. Wu and H. R. Wen, *Inorg. Chem.,* 2013, **52**, 1679; (c) X. G. Liu, H. Wang, B. Chen, Y. Zou, Z. G. Gu, Z. J. Zhao and L. Shen, *Chem. Commun.*, 2015, **51**, 1677.
8. (a) Z. Z. Lu, R. Zhang, Y. Z. Li, Z. J. Guo and H. G. Zheng, *J. Am. Chem. Soc.,* 2010, **133**, 4172; (b) L. G. Beauvais, M. P. Shores and J. R. Long, *J. Am. Chem. Soc.,* 2000, **122**, 2763.
9. (a) O. M. Yaghi and H. Li, *J. Am. Chem. Soc.*, 1996, **118**, 295; (b) T. K. Maji, K. Uemura, H. C. Chang, R. Matsuda and S. Kitagawa, *Angew. Chem. Int. Ed.,* 2004, **43**, 3269; (c) T. Shiga, H. Okawa, S. Kitagawa and M. Ohba, *J. Am. Chem. Soc.,* 2006, **128**, 16426.
10. (a) L. Carlucci, G. Ciani, S. Maggini, D. M. Proserpio and M. Visconti, *Chem.-Eur. J.,* 2010, **16**, 12328; (b) M. C. Bernini, N. Snejko, E. G. Puebla, E. V. Brusau, G. E. Narda and M. A. Monge, *Inorg. Chem.,* 2011, **50**, 5958; (c) M. Yang, F. L. Jiang, Q. H. Chen, Y. F. Zhou, R. Feng, K. C. Xiong and M. C. Hong, *CrystEngComm,* 2011, **13**, 3971.

11. (a) T. Panda, P. Pachfule and R. Banerjee, *Chem. Commun.,* 2011, **47**, 7674; (b) N. Reimer, H. Reinsch, A. K. Inge and N. Stock, *Inorg. Chem.*, 2015, **54**, 492; (c) G. T. Vuong, M. H. Pham and T. O. Do, *Dalton Trans*., 2013, **42**, 550.
12. (a) Q. Liu, L. L. Yu, Y. Wang, Y. Z. Ji, J. Horvat, M. L. Cheng, X. Y. Jia and G. X. Wang, *Inorg. Chem.,* 2013, **52**, 2817; (b) J. J. Gassensmith, J. Y. Kim, J. M. Holcroft, O. K. Farha, J. F. Stoddart, J. T. Hupp and N. C. Jeong, *J. Am. Chem. Soc.*, 2014, **136**, 8277.
13. (a) Z. J. Zhang, L. P. Zhang, L. Wojtas, P. Nugent, M. Eddaoudi and M. J. Zaworotko, *J. Am. Chem. Soc.,* 2012, **134**, 924; (b) M. Saito, T. Toyao, K. Ueda, T. Kamegawa, Y. Horiuchi and M. Matsuoka, *Dalton Trans*., 2013, **42**, 9444.
14. S. L. Zhang, R. F. Chen, J. Yin, F. Liu, H. J. Jiang, N. E. Shi, Z. F. An, C. Ma, B. Liu and W. Huang, *Org. Lett.,* 2010, **12**, 3438.
15. G. M. Sheldrick, *SADABS Siemens Area Correction Absorption Program*, University of Göttingen, Göttingen, Germany, 1994.
16. Bruker 2000, *SMART (Version 5.0)*, *SAINT-plus (Version 6)*, *SHELXTL (Version 6.1)*, *and SADABS (Version 2.03)*, Bruker AXS Inc., Madison, WI.
17. A. L. Spek, Platon Program, *Acta Crystallogr.*, *Sect. A: Fundam. Crystallogr.*, 1990, **46**, 194.
18. V. A. Blatov, A. P. Shevchenko and V. N. Serezhkin, *J. Appl. Crystallogr.*, 2000, **33**, 1193.
19. (a) D. Sarma, K. V. Ramanujachary, S. E. Lofland, T. Magdaleno and S. Natarajan, *Inorg. Chem*., 2009, **48**, 11660; (b) M. Tonigold, Y. Lu, A. Mavrandonakis, A. Puls, R. Staudt, J. Möllmer, J. Sauer and D. Vokmer, *Chem. Eur. J*., 2011, **17**, 8671; (c) B. K. Tripuramallu, P. Manna, S. N. Reddy and S. K. Das, *Cryst. Growth Des*., 2012, **12**, 777.
20. J. Ji, Y. Zhang, Y. F. Yang, H. Xu, Y. H. Wen, *Eur. J. Inorg. Chem.,* 2013, **24**, 4336.
21. (a) O. Fabelo, J. Pasán, L. C. Delgado, F. S. Delgado, A. Labrador, F. Lloret, M. Julve and C. Ruiz-Pérez, *Inorg. Chem.*, 2008, **47**, 8053; (b) J. Y. Wu, S. M. Huang and M. H. Chiang, *CrystEngComm*, 2010, **12**, 3913.

Table 1 Crystal Data and Structure Refinements for Compounds **1-5**.

	1	**2**	**3**	**4**	**5**
Formula	$C_{36}H_{32}CoN_{10}O_{12}$	$C_{35}H_{24}CoF_6N_4O_7$	$C_{104}H_{58}Co_4F_{24}N_8O_{19}$	$C_{32}H_{31}CoN_5O_{10}$	$C_{64}H_{46}Co_2N_8O_{15}$
F_w	855.65	781.51	2415.30	704.47	1284.95
Crystal system	Monoclinic	Monoclinic	Monoclinic	Monoclinic	Monoclinic
Space group	*C*2/*c*	$P2_1/c$	*P*2/*c*	*C*2/*c*	*C*2/*c*
a/Å	17.733(2)	11.8328(9)	16.2799(8)	22.639(7)	25.614(2)
b/Å	8.1319(11)	23.8489(18)	7.2214(4)	22.322(7)	12.2428(12)
c/Å	26.416(4)	13.5413(8)	24.2716(10)	14.117(5)	18.9927(19)
β/°	101.854(2)	120.368(5)	116.419(3)	108.630(5)	112.679(2)
V/Å^3	3728.0(9)	3297.0(4)	2555.5(2)	6760(4)	5495.4(9)
Z	4	4	1	8	4
D_c/g cm^{-3}	1.524	1.574	1.569	1.243	1.553
F(000)	1764	1580	1214	2600	2640
R(int)	0.0169	0.0614	0.0164	0.0794	0.0623
GOF on F^2	1.055	1.074	1.023	1.049	1.056
$R_1[I>2\sigma(I)]$	0.0450	0.0484	0.0321	0.0839	0.0537
wR_2 (all data)	0.1421	0.1587	0.1020	0.2424	0.1494

$R_1 = \Sigma||F_o| - |F_c||/\Sigma|F_o|$, $wR_2 = \{\Sigma[w(F_o^2 - F_c^2)^2]/[w(F_o^2)^2]\}^{1/2}$, where $w = 1/[\sigma^2(F_o^2) + (aP)^2 + bP]$, $P = (F_o^2 + 2F_c^2)/3$.

Graphical Abstract

Solvent-Induced Synthesis of Cobalt(II) Coordination Polymers Based on a Rigid Ligand and Flexible Carboxylic Acid Ligands: Syntheses, Structures and Magnetic Properties

Ting Wang, Chuanlei Zhang, Zemin Ju and Hegen Zheng*

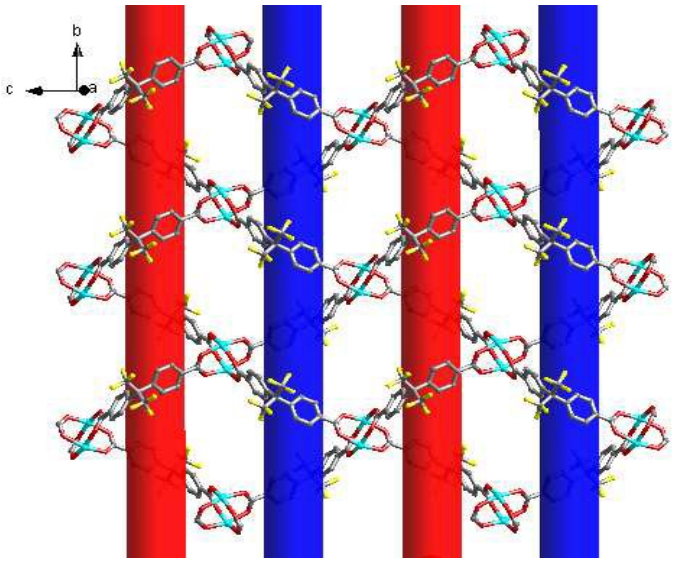

The structural formations for compounds **1-5** are effected by using different solvents or different carboxylic acid ligands.